Adaptive Fuzzy Connectedness-Based Medical Image Segmentation

Amol Pednekar Ioannis A. Kakadiaris Uday Kurkure
Visual Computing Lab, Dept. of Computer Science, Univ. of Houston, Houston, TX, USA
apedneka@bayou.uh.edu ioannisk@uh.edu ukurkure@bayou.uh.edu

Abstract

In this paper, we present an enhancement of the fuzzy connectedness-based image segmentation method based on dynamic computation of adaptive weights for the homogeneity and the directional gradient energy functions. Adaptive weights enhance the performance and robustness of the conventional fuzzy connectedness-based segmentation while decreasing the degree of user interaction. The accuracy of the adaptive fuzzy connectedness-based segmentation of typical fuzzy medical images is assessed with respect to the conventional fuzzy connectedness.

1. Introduction

Medical image computing has revolutionized the field of medicine by providing novel methods to extract and visualize information from medical data, acquired using various acquisition modalities. Image segmentation is one of the most important steps as in the analysis of the preprocessed patient image data, which can help in diagnosis, treatment planning, as well as treatment delivery. The main goal of the segmentation process is to divide an image into parts that have a strong correlation with objects or areas of the real world depicted in the image. Thus, segmented images make any abnormalities in the tissue distinctly visible. Hard or binary segmentation techniques have been the focus of research for many decades. However, medical images are *fuzzy*, they are characterized as a composition of signal intensities specific to different tissue types, noise, blurring, background variation, partial voluming, and certain acquisition-specific effects (e.g., surface coil intensity fall off in MR imaging). Moreover, anatomical objects in medical data are characterized by certain intensity features and patterns of intensity variations. Thus, medical image segmentation requires more complex classification basis than merely intensity values.

The fuzzy connectedness-based image segmentation framework developed by Udupa and his collaborators [6, 7] assigns fuzzy affinities to the target object as compared to hard binary classification. The affinity is computed as the weighted sum of the intensity and the intensity gradient in the neighborhood of the pixel to capture the intensity features and patterns of intensity variations. However, this framework assumes user selected values for the associated weights. Thus, the resultant fuzzy connectedness map is sensitive to the combination of features of the target region and the selected weight.

In this paper, we propose employing dynamically computed adaptive weights for the homogeneity and the gradient energy functions, thus decreasing user interaction. Since the adjacency of a pixel to the seed pixel in intensity and gradient space depends on the location of the pixel relative to target region centroid, adaptive weights introduce shift-variance to the definition of fuzzy connectedness. In addition, we employ the direction of the gradient along with its magnitude, which gives importance to variations in intensity in a specific direction. The remainder of the paper is organized as follows: In Section 2, we provide a brief overview of the conventional fuzzy connectedness-based image segmentation. Section 3 provides details of our modifications to the conventional fuzzy connectedness-based fuzzy segmentation. We present a comparison study of the adaptive weights fuzzy connectedness with respect to conventional fuzzy connectedness in Section 4. Finally, Section 5 summarizes out findings.

2. Fuzzy Connectedness

The Fuzzy Connected Image Segmentation framework developed by Udupa and his collaborators [6, 7] assigns fuzzy affinities to the target object during classification, which are used for the segmentation of the target object in the image. The affinity between the two given pixels (or voxels) in an image (or a volume) is defined as a combined weighted function of the degree of coordinate space adjacency, the degree of intensity space adjacency, and the degree of intensity gradient space adjacency to the corresponding target object features. The goal is to capture the specific intensity patterns attached to the object of interest.

Notation: A binary scene over a fuzzy digital space (Z^n, α) is a pair $\varsigma = (C, f)$, where C is a n-dimensional array of spels (spatial elements - pixels or voxels) and f is a

*This material is based upon work supported by the Texas Higher Education Coordinating Board (Grant No. ARP003652-0010-1999) and by the National Science Foundation (Grant No. CISE/HRA 9985482).

function whose domain is C, called the scene domain, and whose range is a subset of the closed interval $[0, 1]$. Fuzzy affinity k is any reflexive and symmetric fuzzy relation in C, that is [6]:

$$\begin{array}{l} k = \{((c,d), \mu_\kappa(c,d)) | (c,d) \in C\} \\ \mu_\kappa : C \times C \rightarrow [0,1] \\ \mu_\kappa(c,c) = 1, \forall c \in C \\ \mu_\kappa(c,d) = \mu_\kappa(d,c), \forall (c,d) \in C \ . \end{array} \quad (1)$$

The general form of μ_κ can be written as follows: $\mu_\kappa(c,d) = h(\mu_\alpha(c,d), \mu_\psi(c,d), \mu_\phi(c,d), c, d) \ \forall (c,d) \in C$, where: $\mu_\alpha(c,d)$ represents the degree of coordinate space adjacency of c and d; μ_ψ represents the degree of intensity space adjacency of c and d; and μ_ϕ represents the degree of intensity gradient space adjacency of c and d to the corresponding target object features. Fuzzy k-connectedness K is a fuzzy relationship in C, where $\mu_\kappa(c,d)$ is the strength of the strongest path between c and d, and the strength of a path is the smallest affinity along the path. A fuzzy connected component is defined as a hard binary relationship K_θ in C based on the fuzzy k-connectedness:

$$\mu_\kappa(c,d) = \begin{cases} 1 & \text{iff } \mu_\kappa(c,d) \geq \theta \in [0,1] \\ 0 & otherwise. \end{cases} \quad (2)$$

Let O_θ be an equivalence class [4] of the relation K_θ in C. A fuzzy k-component Γ_θ of C of strength θ is a fuzzy subset of C defined by the membership function [6]:

$$\mu_{\Gamma_\theta} = \begin{cases} f(c) & \text{iff } c \in O_\theta \\ 0 & otherwise. \end{cases} \quad (3)$$

The equivalence class $O_\theta \subset C$, such that for any $(c,d) \in C$, $\mu_\kappa(c,d) \geq \theta$, $\theta \in [0,1]$, and for any $e \in \{C - O_\theta\}$, $\mu_\kappa(c,d) < \theta$. The notation $[O]_\theta$ is used to denote the equivalence class of K_θ that contains O for any $O \in C$. The fuzzy k-component of C that contains O, denoted $\Gamma_\theta(O)$, is a fuzzy subset of C whose membership function is given by:

$$\mu_{\Gamma_{\theta(O)}} = \begin{cases} f(c) & \text{iff } c \in [O]_\theta \\ 0 & otherwise. \end{cases} \quad (4)$$

A fuzzy $k\theta$-object of ς is a fuzzy k-component of ς of strength θ. For any spel $O \in C$, a fuzzy $k\theta$-object of ς that contains O is a fuzzy k-component of ς of strength θ that contains O. Given k, O, θ, and ς, a fuzzy $k\theta$-object of ς of strength $\theta \in [0,1]$ containing O, for any $O \in C$, can be computed via dynamic programming [7].

Fuzzy Connectedness-based Segmentation: In a generic implementation of fuzzy connectedness for $c, d \in C$:$\mu_\kappa(c,d) = h(\mu_\alpha(c,d), f(c), f(d), c, d)$, where c, d are the image locations of the two pixels, $\mu_\alpha(c,d)$ is an adjacency function based on the distance of the two pixels,

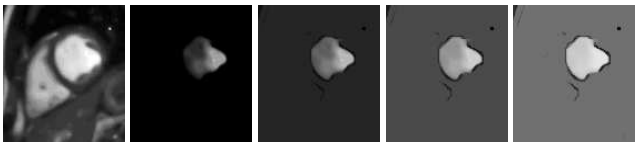

(a) (b) (c) (d) (e)

Figure 1: Fuzzy affinity maps of short-axis cardiac MRI (a), for which the weight for intensity energy function is (b) 1.0, (c) 0.75, (d) 0.50, and (e) 0.25, respectively.

and $f(c)$ and $f(d)$ are the intensity of pixels c and d, respectively. In this general form, $\mu_\kappa(c,d)$ is shift-variant. In other words, it is dependent on the location of pixels c and d. A more specific and shift-invariant definition for a fuzzy affinity was introduced in [6]:

$$\begin{array}{l} \mu_\kappa(c,d) = \mu_\alpha(c,d)[\omega_1 h_1(f(c), f(d)) \\ \qquad\qquad + \omega_2 h_2(f(c), f(d))], \\ \mu_\kappa(c,c) = 1 \end{array} \quad (5)$$

where, $\mu_\kappa(c,d)$ is a linear combination of $h_1(f(c), f(d))$ and $h_2(f(c), f(d))$, with $w_1 + w_2 = 1$. The three features taken into consideration are: the adjacency between the pixels $\mu_\alpha(c,d)$, the intensity of the pixels $h_1(f(c), f(d))$, and the gradient of the pixels $h_2(f(c), f(d))$.

The adjacency function $\mu_\alpha(c,d)$ is assumed to be a hard adjacency relation, such that:

$$\mu_\alpha(c,d) = \begin{cases} 1 & if \quad \sqrt{\sum_i (c_i - d_i)^2} \leq 1 \\ 0 & if \quad otherwise \ , \end{cases} \quad (6)$$

where c_i $(0 \leq i \leq n)$ are the pixel's coordinates in n dimensions. The functions h_1 and h_2 are Gaussian functions of $\frac{1}{2}(f(c) + f(d))$ and $|f(c) - f(d)|$, respectively, such that:

$$\begin{array}{l} h_1(f(c), f(d)) = e^{-\frac{1}{2}[\frac{\frac{1}{2}(f(c)+f(d))-m_1}{s_1}]^2} \\ h_2(f(c), f(d)) = e^{-\frac{1}{2}[\frac{(|f(c)-f(d)|)-m_2}{s_2}]^2} \end{array} \quad (7)$$

where m_1 and s_1 are the mean intensity and standard deviation of the intensity of the sample region and m_2 and s_2 are the mean and standard deviation of the gradient of the sample region.

3. Adaptive Fuzzy Connectedness

With ω_1 and ω_2 kept as free parameters, the results obtained from fuzzy connectedness remain highly sensitive to the selection of the weight values. Fig. 1 depicts how the affinities attached to pixels vary. Note that a higher weight for the intensity energy function fails to capture the fall in intensity from right to left. However, this falloff is captured better as the weight for gradient energy function increases

and attaches more and more uniform affinity values over the target region, while enhancing the boundary. One may manually adjust these weights in order to find the most suitable combination, but this does not help the cause of automatic or minimal user interaction segmentation. To that end, we have developed a method to adapt these weights dynamically. Specifically, we compute ω_1 and ω_2 as adaptive parameters depending on the ratio of homogeneity and gradient function values at each spel location, as follows: $\omega_1 = \frac{h_1}{(h_1+h_2)}$ and $\omega_2 = 1 - w_1$.

We have kept α as the hard adjacency relationship (i.e., 4-adjacency for n=2 and 6-adjacency for n=3). To improve the accuracy of computation of the intensity gradient space adjacency, we incorporate gradient information from all n directions. This directional gradients method captures the gradual change in intensity in one direction, typical in medical images, much better than the simple mean gradient as depicted in Figs. 2(b,c). Our method of weight assignment takes advantage of the fact that the closer the spel is to the center of the target object the higher will be the degree of intensity space adjacency as compared to when the spel is near the boundary of the target. As the spel moves towards the boundary automatically more weight is assigned to the degree of adjacency in intensity gradient space, thus enabling more accurate boundary definition. As it can be seen from Fig. 2(d), depicting the result using adaptive weights fuzzy connectedness with directional gradients, our proposed method enhances the values of affinity attached to the pixels of the target object, and thus resulting in better defined fuzzy objects. This is accomplished without involving the user to find the best possible combination of ω_1 and ω_2. Fig. 4 depicts the improvements achieved by these extensions and modifications. As our refined fuzzy connectedness attaches much higher and uniform affinities to the target object relative to rest of the image, the edge magnitudes of fuzzy connectedness images are pronounced which is crucial for further automation of the segmentation of the target object. As can be seen from Fig. 2(j), a valley between the target region and the rest of the image in affinity image histogram is broadened by the adaptive fuzzy connectedness compared to conventional fuzzy connectedness. This valley can be detected easily by Otsu's auto thresholding algorithm [3]. This automatic threshold detection of the target region relieves the user of deciding threshold of affinity map for object extraction. The only manual interaction left is the selection of the seed pixel.

3.1. Fuzzy Object Extraction Algorithm

In this section, we present the modified algorithm for adaptive n-fuzzy object extraction.

Adaptive κFOE algorithm

Input: ς, o, and κ, as defined previously in section **??**.
Output:$K_o - scene$ of ς, denoted ς_o.

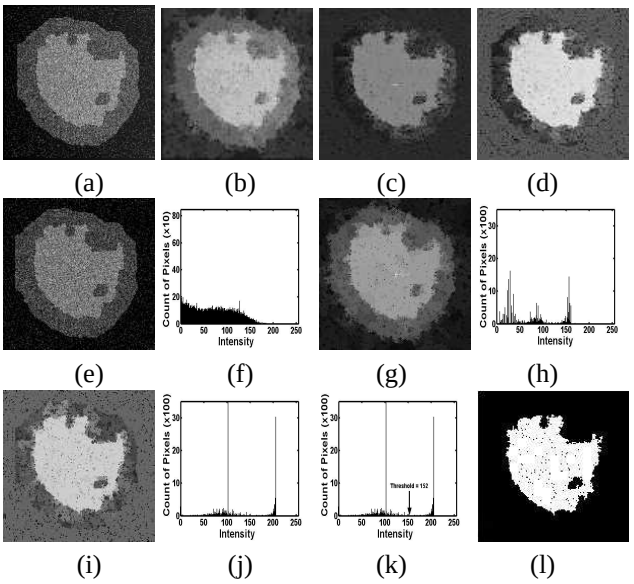

Figure 2: Fuzzy affinity values are mapped to gray scale (0-255) using the value 0.5 as the weight for the intensity energy function. (a) a synthetic image and the resultant affinity maps for (b) the mean gradient, (c) the directional gradient, and (d) the adaptive weights directional gradient method, respectively. (e) Sample noisy image from the phantom dataset and (f) corresponding histogram. The affinity map for (g) the conventional fuzzy connectedness method and (h) the resultant histogram. The affinity map for (i) the adaptive fuzzy connectedness and (j) the resultant histogram. (k) Automatically detected threshold value for the affinity image and (l) the resultant thresholded image.

Auxiliary Data Structures: An nD array representing the $K_o - scene\ \varsigma_o = (C_o, f_o)$ of ς and a queue Q of spels.
Pseudo code:
set all elements of ς_o to 0 except o which is set to 1;
  push all spels $c \in \varsigma_o$ such that $\mu_\kappa(o, c) > 0$ to Q;
  while Q is not empty do{
    remove a spel c from Q;
    find $f_{\max} = \max_{d \in \mathcal{C}_o}[\min(f_o(d), \mu_\kappa(c, d))]$;
    if $f_{\max} > f_o(c)$ {
      set $f_o(c) = f_{\max}$;
      push all spels e such that $\mu_\kappa(c, e) > 0$ to Q;
    }
  }

The fuzzy affinity $\mu_\kappa(c, d)$ is computed as:

$$\begin{aligned} &\mu_\kappa(c, d) = \mu_\alpha(c, d)[\tfrac{h_1^2}{h_1+h_2} + \tfrac{h_2^2}{h_1+h_2}], \\ &\mu_\kappa(c, c) = 1 \end{aligned} \tag{8}$$

and the gradient energy function is given by:

$$h_2(f(c), f(d)) = e^{-\frac{1}{2}[\frac{(|f(c)-f(d)|)-m_{d(c,d)}}{s_{d(c,d)}}]^2} \tag{9}$$

where $m_{d(c,d)}$ and $s_{d(c,d)}$ are the mean and standard deviation of the intensity gradient of the sample region in the direction from c to d.

4. Performance Evaluation

In this section, first we present the results of the adaptive fuzzy connectedness segmentation algorithm on a phantom data set. Next, the adaptive fuzzy segmentation algorithm results will be compared to the results of the conventional fuzzy connectedness-based segmentation. Finally, we present the results of the fuzzy segmentation algorithm on actual MR data.

One of the main challenges with medical data is that the ground truth cannot be exactly defined. To overcome this problem, we have created a phantom data set where the ground truth is already known. Testing a segmentation algorithm on a phantom data set allows for the establishment of a ground truth and the definition of a metric. This type of testing does not take into account the inter- and intra-rater variations that result in a less than a gold standard in the realistic world of medical imaging. However, the use of a phantom data set allows for an analysis of the technique to decide if, it is worthy of more arduous testing on real data. The phantom images contain similar intensities of a medical image and posses varying degrees of blur, noise, and background intensity variation. In fact, these three variations will serve as the parameters to assess the robustness of the adaptive fuzzy connectedness-based segmentation algorithm for medical image data.

Noise and blurring are always present in image acquisition; most especially in medical image acquisition as a result of the inaccuracies imposed by the nature of the scanners. A background intensity variation has been added to account for a common issue in medical images in which a shift in intensity variation from one side of the image to another may cause the region of interest, if it is a large enough region, to consist of significantly different intensity levels. This causes a problem for most segmentation algorithms that are solely based on segmenting the region of interest by its intensity characteristics. The inhomogeneity of the most tissue types in the human body and partial voluming adds to these effects. The goal is to explore the results of the adaptive fuzzy connectedness-based segmentation algorithm on the phantom data sets to determine if this algorithm is well suited for medical images and compare it with the conventional fuzzy connectedness-based segmentation.

A phantom data set was developed, $P = \{C_i | C_i = (C, f), 1 \leq i \leq 60\}$, where each C_i is 150 x 150 pixels and possesses a region of interest similar in structure to that of a short-axis MR-scan of a left ventricle. With this original image, a total of 60 phantom images were created by adding four varying degrees of Gaussian blurring, five varying degrees of zero-mean Gaussian white noise, and two degrees of background variation. The Gaussian blurring was implemented using Gaussian blur filter with a kernel size of five, in order of increasing blur levels $B_0 : \sigma = 0$; $B_1 : \sigma = 0.25$; $B_2 : \sigma = 0.5$; $B_3 : \sigma = 0.75$; and $B_4 : \sigma = 1.0$. The zero-mean Gaussian white noise was implemented as follows: $N_0 : \sigma = 0$; $N_1 : \sigma = 0.001$; $N_2 : \sigma = 0.003$; $N_3 : \sigma = 0.005$; $N_4 : \sigma = 0.007$; and $N_5 : \sigma = 0.01$. The five degrees of blur and six degrees of noise create a total of thirty possible combinations which will be called set BV_0, such that $BV_0 = \{C_i | C_i \subset P, 1 \leq i \leq 30\}$. In addition, a new set of thirty phantoms possessing the same levels of blur and noise but containing an added background variation were created. We call this set of thirty images set BV_1, such that $BV_1 = \{C_i | C_i \subset P, 31 \leq i \leq 60\}$. The background variation was implemented using a slow varying ramp such that 0 was added to the first column and 30 was added to the last column. Figs. 3(a-d) depict examples from the phantom data set. First, we will demonstrate how the adaptive fuzzy connectedness-based segmentation compares to a simple method of thresholding. In order to objectively compute the best possible threshold we define figures of merit for the accuracy of segmentation as follows [5]: For any scene $\mathcal{C} = (C, f)$, we denote by $\mathcal{C}^t = (C, f^t)$ the binary scene which results from thresholding $\mathcal{C}$ at t. That is for any $c \in C$

$$f^t(c) = \begin{cases} 1 & if \quad f^t \geq t \\ 0 & if \quad otherwise. \end{cases} \tag{10}$$

For the accuracy of segmentation, we define a figure of merit (FOM), such that:

$$FOM = \max \left[\left(1 - \frac{|C^t \otimes C_G|}{|C|} \right) \times 100 \right], \tag{11}$$

where C_G represents the ground truth, $|C|$ is the cardinality of C, $\otimes$ represents the exclusive-OR operation, and $|C^t \otimes C_G|$ denotes the number of 1-valued pixels in $C^t \otimes C_G$.

Four different metrics on the fuzzy segmented objects are analyzed in order to delineate the robustness of the adaptive fuzzy connectedness-based segmentation algorithm. The four measures include the computation of the overlap ratio, the computation of the confusion matrix, the computation of the Hausdorff distance, and the computation of the average distance. A new validation software, VALMET [2], was employed to perform the comprehensive quantitative evaluations of the algorithm. The overlap experiments measure the false negatives, false positives, true negatives, and true positives compared to the ground truth, and compute the overlap ratio between ground truth and ROI. The overlap allows us to take into consideration the spatial information by classifying the degree of overlap, making it a superior measure of segmentation quality as compared to

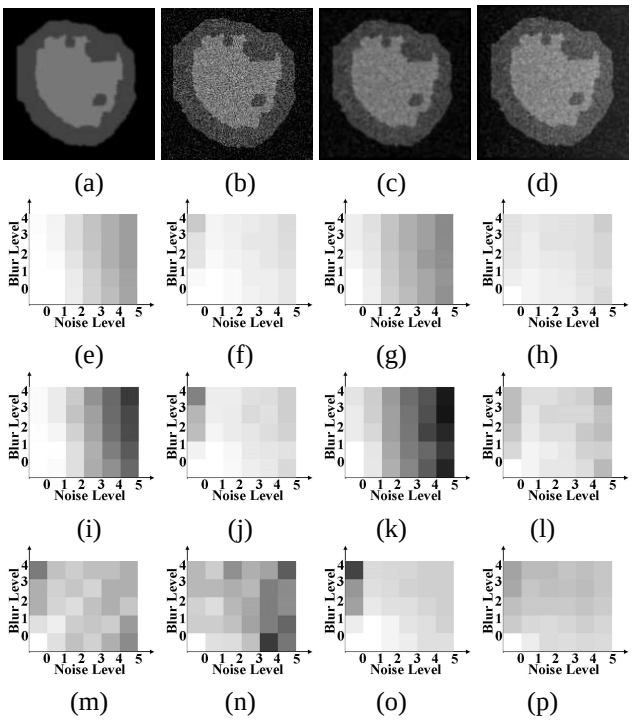

Figure 3: Examples from the phantom data set P obtained by varying the following parameters: (a) blur, (b) noise, (c) blur + noise and, (d) blur + noise + background variation. The overlap ratios mapped to gray scale (0-255) for the thresholded (e,g) and the fuzzy segmented (f,h) sets BV_0 and BV_1, respectively. $\mathcal{M}_{ij}$ errors mapped to gray scale (255-0) for the thresholded (i,k) and the fuzzy segmented (j,l) sets BV_0 and BV_1, respectively. Hausdorff distance metric (m,n) and average distance metric (o,p) mapped to gray scale (0-255) for sets BV_0 and BV_1, respectively.

the mean and standard deviation. Intuitively, a larger degree of overlap signifies a better segmentation. Fig. 3(e-h) presents the measured overlap ratio obtained with VALMET. The overlap measurement study quantitatively indicates that the fuzzy segmentation performs significantly better than threshold with complex images achieving 90% overlap results, where thresholding can achieve at most 70% overlap. To analyze more specifically the degree of misclassification, we need to measure which pixels are classified incorrectly and which are classified correctly. This leads us to the confusion matrix analysis.

The confusion matrices delineate the number of pixels that were classified as the background and ROI, both correctly and incorrectly. Let $\mathcal{M}$ be a confusion matrix of dimension N, where $\mathcal{M}_{ij}$ is an element and $0 \leq i \leq N, 0 \leq j \leq N$. The multi-class Type I error ($\mathcal{M}_{ij}$) is defined as:

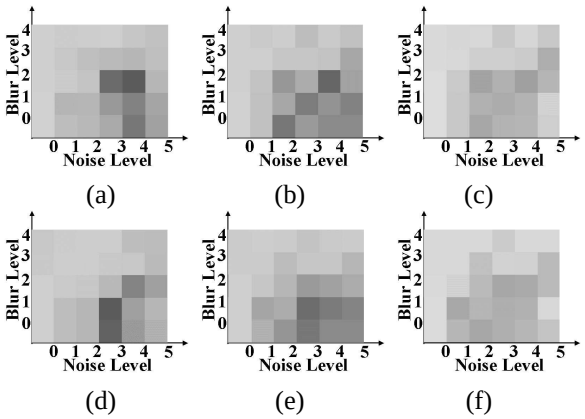

Figure 4: The mean intensity values of the segmented region of interest mapped to gray scale (0-255) for the conventional fuzzy connectedness method using the value 0.5 as the weight for the intensity energy function with (a,d) mean gradient, (b,e) directional gradient, and (c,f) adaptive weights with directional gradients for the sets BV_0 and BV_1, respectively.

$M_I^{(k)} = 100 \times \frac{\left[\left(\sum_{i=0}^{N} \mathcal{M}_{ik}\right) - \mathcal{M}_{kk}\right]}{\left[\sum_{i=0}^{N} \mathcal{M}_{ik}\right]}$, where the numerator represents the number of voxels of class k not classified as k and the denominator is the total number of voxels of class k. The M_I errors for ROI and background are summed to give a measure of error of misclassification. Figs. 3(i-l) represent the sum of the M_I errors for the threshold and fuzzy segmentations of the sets BV_0 and BV_1. It is obvious from examining the matrices that as the complexity of the image increases, the degree of misclassification becomes significantly higher in the threshold segmentation than in the fuzzy segmentation. This shows that adaptive fuzzy connectedness-based segmentation is robust to increasing image complexity.

The Hausdorff distance measures the distance between the boundaries of segmented objects. Figs. 3(m,n) depict the Hausdorff distance between the fuzzy segmented ROI and the gold standard for varying degrees of intensity variation, noise, and blurring. A Hausdorff distance of 0 signifies that the two boundaries have a maximum directed Hausdorff distance of 0 between them. In other words, they are equal. Increasing Hausdorff distances signify increasing distance between the two boundaries. As the complexity of the image increases, the distance between the fuzzy segmented ROI and the gold standard increases.

Unlike the Hausdorff distance, the mean absolute distance calculates the average of two boundaries. Once the average boundary is found, the average distance is calculated. The advantages of this metric are that the average distance

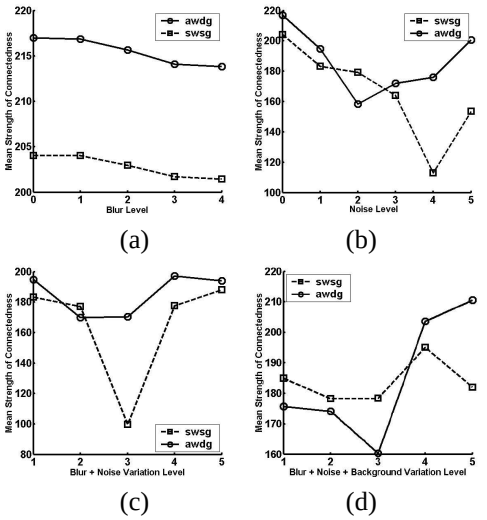

Figure 5: Comparative plots of the mean intensity values of the segmented region of interest for different levels of (a) blur, (b) noise, (c) blur+noise, and (d) blur+noise+background variation, respectively.

calculated may give a more accurate picture than the Hausdorff metric. Since in certain cases, set of boundaries dissimilar only over small portions may have the same Hausdorff distance as that of globally dissimilar set of boundaries [1]. Additionally, the average surface distance is not sensitive to the size of the object as the volumetric overlap is [2, 1]. These metrics are more intuitive because they result in one number, a distance, which shows the difference between two contours.

We use the mean values of the strength of connectedness attached to the ground truth as metric to compare the performance of adaptive fuzzy connectedness-based segmentation using directional gradients with respect to conventional fuzzy connectedness-based segmentation. Fig. 5 shows the results of comparison study between the conventional fuzzy connectedness-based segmentation and adaptive fuzzy connectedness-based segmentation using directional gradients on the phantom data set. The mean intensity values of the segmented region of interest (Figs. 4(a-f)) show that the introduction of directional gradients and the adaptive weights make segmentation more robust to noise and background variation. Figs. 5(a-d) depict consistently better performance of the adaptive fuzzy connectedness over the conventional fuzzy connectedness. Figs. 6(a-i) depict the results of the adaptive connectedness method applied to medical images.

5. Conclusion

In summary, our proposed method (which dynamically computes adaptive weights for the intensity homogeneity and the directional intensity gradient energy functions) enhances the performance and robustness of the conventional fuzzy connectedness-based segmentation while decreasing the degree of user interaction.

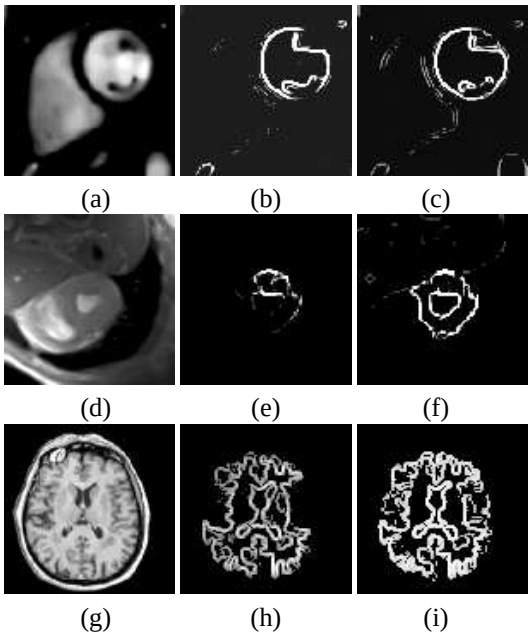

Figure 6: Results of the conventional fuzzy connectedness method (b,e,h) and the adaptive fuzzy connectedness method (c,f,i) applied to medical images (a,d,g).

References

[1] V. Chalana and Y. Kim. A Methodology for Evaluation of Boundary Detection Algorithm on Medical Images. In *IEEE Trans on Medical Imaging*, volume 16, pages 642–652, 1997.

[2] G. Gerig, M. Jomier, and M. Chakos. VALMET: A New Validation Tool for Assessing and Improving 3D Object Segmentation. In *MICCAI*, pages 516–523, 2001.

[3] N. Otsu. A Threshold Selection Method from Gray-Level Histograms. In *IEEE Transactions on Systems, Man, and Cybernetics*, volume SMC-9, pages 62–66, January 1979.

[4] F. Preparata and M. Shamos. *Computational Geometry*. Springer, 1985.

[5] P. K. Saha, J. K. Udupa, and D. Odhner. Scale-based Fuzzy Connected Image Segmentation: Theory, Algorithms, and Validation. *Computer Vision and Image Understanding*, 77:145–174, 2000.

[6] J. Udupa and S. Samarasekera. Fuzzy Connectedness and Object Definition: Theory, Algorithms, and Applications in Image Segmentation. *Graphical Models and Image Processing*, 58(3):246–261, 1996.

[7] J. K. Udupa and S. Samarasekera. Fuzzy Connectedness and Object Definition. In *SPIE Proceedings Medical Imaging*, volume 2431, pages 2–10. SPIE, 1995.